Quantum phases of Bose gases on a lattice with pair-tunneling*

Wang Yue-Ming(王月明)† and Liang Jiu-Qing(梁九卿)

Department of Physics, Institute of Theoretical Physics, Shanxi University, Taiyuan 030006*, China*

(Received 12 February 2012; revised manuscript received 21 March 2012)

We investigate the strongly interacting lattice Bose gases on a lattice with two-body interaction of nearest neighbors characterized by pair tunneling. The excitation spectrum and the depletion of the condensate of lattice Bose gases are investigated using the Bogoliubov transformation method and the results show that there is a pair condensate as well as a single particle condensate. The various possible quantum phases, such as the Mott-insulator phase (MI), the superfluid phase (SF) of an individual atom, the charge density wave phase (CDW), the supersolid phase (SS), the pair-superfluid (PSF) phase, and the pair-supersolid phase (PSS) are discussed in different parametric regions within our extended Bose–Hubbard model using perturbation theory.

Keywords: Bose–Einstein condensate, quantum phase, optical lattice, superfluidity

PACS: 03.75.Lm, 64.70.Tg, 67.85.Hj **DOI:** 10.1088/1674-1056/21/6/060305

1. Introduction

In the past few years the experimental manipulation of neutral atoms in optical lattices has achieved fascinating progress[1−4] that has opened up a way to simulate the quantum complex systems of condensed matter physics, such as high-T_c superconductors, Hall systems, and superfluid ^{4}He, ascribed to the extreme flexibility and controllability of atom-optical systems.[5] For the atoms confined in different lattice sites it is possible to tune the interatomic interactions with great precision by adjusting the strength of the periodic potential and to enhance the interactions well into the strong regime, even in the dilute limit. Bose–Hubbard model (BHM) has been proven to be the most successful model describing ultra-cold atomic gases loaded into optical lattices.[6] This model has three terms:[7] a kinetic energy term which allows atom tunneling between nearest-neighbor lattice sites, a potential energy of on-site two-body interaction, and a chemical potential term which fixes the number of atoms. We point out that in the strong coupling regime with a large ratio U/J the usual on-site approximation of two-body interaction within BHM ought to be extended to include nearest-neighbor sites. The nearest-neighbor (NN) interactions result in a new tunneling mechanism, e.g., pair-tunneling different from the so-called second order tunneling process which can be obtained by the second order perturbation theory,[8−12] and cannot be neglected even though they are much smaller than the on-site interaction itself. Thus an extended Bose–Hubbard model (EBHM) characterized by an atom-pair tunneling term in a double-well trap was derived in Ref. [8] showing a perfect agreement with the experimental observation of two-atom correlated tunneling.[9] For a deep-enough lattice the pair-tunneling can be the dominant process.[12] Recently the electron pair-tunneling process has been paid much attention in condensed physics.[13−15] An optical realization of correlated pair tunneling of two interacting bosons in a double-well potential was proposed.[16] Following our previous work, in which we investigated repulsive bound-atom pairs in an optical lattice with two-body interaction of the nearest neighbors,[17] we investigate the quantum lattice gas within our EBHM in strong coupling regime.

The paper is organized as follows. In Section 2, we introduce the model Hamiltonian. We study the depletion of the condensate and the excitation spectrum of lattice Bose gases using the Bogoliubov approach in Section 3. In Section 4 we obtain rich phase diagrams within the EBHM using perturbative theory under different parametric conditions. Finally we present a brief summary of our conclusions and discuss

*Project supported by the National Natural Science Foundation of China (Grant Nos. 11075099, 10974124, and 11105087).

†Corresponding author. E-mail: wang_ym@sxu.edu.cn

© 2012 Chinese Physical Society and IOP Publishing Ltd

the experimental observability in the last section.

2. The extended Bose–Hubbard model

The dynamics of an atomic Bose–Einstein condensate (BEC) loaded into the lowest band of a sufficiently deep optical lattice is well described by a single-band EBHM with Hamiltonianin[8]

$$\begin{aligned} H = & -\sum_i \mu n_i - \sum_i [J_0 - U_3(n_i + n_{i+1} - 1)] \\ & \times (a_i^\dagger a_{i+1} + a_{i+1}^\dagger a_i) + \frac{U_0}{2}\sum_i a_i^\dagger a_i^\dagger a_i a_i \\ & + (U_1 + U_2)\sum_i a_i^\dagger a_{i+1}^\dagger a_{i+1} a_i \\ & + \frac{U_2}{2}\sum_i (a_i^\dagger a_i^\dagger a_{i+1} a_{i+1} + a_{i+1}^\dagger a_{i+1}^\dagger a_i a_i), \quad (1) \end{aligned}$$

where a_i is the i-th site boson annihilation operator and $n_i = a_i^\dagger a_i$ is the corresponding atom-number operator. μ is the chemical potential needed to fix the average total number of bosons in the lattice. The new coupling constants between atoms on neighboring lattice-sites are given by

$$\begin{aligned} U_1 = & \int w_i(x_2) w_{i+1}(x_1) U(|x_1 - x_2|) \\ & \times w_{i+1}(x_1) w_i(x_2) \mathrm{d}x_1 \mathrm{d}x_2, \\ U_2 = & \int w_i(x_2) w_i(x_1) U(|x_1 - x_2|) \\ & \times w_{i+1}(x_1) w_{i+1}(x_2) \mathrm{d}x_1 \mathrm{d}x_2, \\ U_3 = & \int w_i(x_2) w_{i+1}(x_1) U(|x_1 - x_2|) \\ & \times w_{i+1}(x_1) w_{i+1}(x_2) \mathrm{d}x_1 \mathrm{d}x_2, \quad (2) \end{aligned}$$

where $U(|x_1 - x_2|)$ is the two-atom interaction potential and w_i denotes Wannier wave functions. U_0 is the usual on-site atom-interaction strength, and the fourth term relating to U_1 denotes the nearest-neighbor repulsion, which has been given in various lattice models in the literature, while the U_2 part is new. The conceptually new transition-matrix element relating to $U_2/2$ describes obviously the atom-pair tunneling. The atom–atom interaction including the nearest-neighbor results in an additional Josephson tunneling term depending on the coupling constant U_3 and the atom-number operator $n_i + n_{i+1} - 1$. This term as a matter of fact suppresses the nearest-neighbor tunneling. The coupling constants U_1, U_2, and U_3 are much smaller comparing with U_0. Although the value of U_2 compared with the on-site interaction is small, it plays a crucial role in the strong interaction regime.

3. Bogoliubov approach

We first transform Hamiltonian (1) to momentum space by introducing creation and annihilation operators $a_{\boldsymbol{K}}^\dagger$ and $a_{\boldsymbol{K}}$, respectively, such that

$$\begin{aligned} a_i^\dagger &= \frac{1}{\sqrt{N_\mathrm{s}}}\sum_{\boldsymbol{K}} a_{\boldsymbol{K}}^\dagger \exp(\mathrm{i}\boldsymbol{K}\cdot\boldsymbol{R}_i), \\ a_i &= \frac{1}{\sqrt{N_\mathrm{s}}}\sum_{\boldsymbol{K}} a_{\boldsymbol{K}} \exp(-\mathrm{i}\boldsymbol{K}\cdot\boldsymbol{R}_i), \quad (3) \end{aligned}$$

where N_s is the number of lattice sites and $\boldsymbol{R}_i$ is the coordinate of site i. The wavevector $\boldsymbol{K}$ runs only over the first Brillouin zone. For mathematical convenience we take only a finite volume V, so that the momenta $\hbar\boldsymbol{K}$ are discretized, which allows us to write sums instead of integrals in Eq. (3). Later we will take the continuum limit $V \to \infty$. Using the fact that $\sum_i \exp[-\mathrm{i}(\boldsymbol{K} - \boldsymbol{K}')\cdot\boldsymbol{R}_i] = N_\mathrm{s}\delta_{\boldsymbol{K},\boldsymbol{K}'}$, the prefactor $1/\sqrt{N_\mathrm{s}}$ inserted ensures that the total number of particles satisfies $N = \sum_i a_i^\dagger a_i = \sum_{\boldsymbol{K}} a_{\boldsymbol{K}}^\dagger a_{\boldsymbol{K}}$. For a Bose condensed gas the average number of condensate atoms N_0 is a number much larger than one, which means that $N_0 = \langle a_{\boldsymbol{0}}^\dagger a_{\boldsymbol{0}}\rangle \approx \langle a_{\boldsymbol{0}} a_{\boldsymbol{0}}^\dagger\rangle$ and such that we can write $N_0 = \langle a_{\boldsymbol{0}}^\dagger\rangle\langle a_{\boldsymbol{0}}\rangle$ and $\langle a_{\boldsymbol{0}}^\dagger\rangle = \langle a_{\boldsymbol{0}}\rangle = \sqrt{N_0}$ assumed to be real. Using the Bogoliubov approximation adopted in Refs. [22] and [23], we obtain the following effective Hamiltonian H_eff

$$\begin{aligned} H_\mathrm{eff} = & \left(-\frac{1}{2}U_0 n_0 - U_1 n_0 - \frac{3}{2}U_2 n_0 - \frac{1}{2}U_3 n_0\right) N_0 \\ & + {\sum_{\boldsymbol{K}}}' \Big\{ \Big[-\mu - \bar{\epsilon}_{\boldsymbol{K}} + 2U_0 n_0 + 2(U_1 + U_2) n_0 \\ & + 2U_2 n_0 \bar{\epsilon}_{\boldsymbol{K}}/J_0 + 4 n_0 U_3 (2 + \bar{\epsilon}_{\boldsymbol{K}}/J_0) \Big] a_{\boldsymbol{K}}^\dagger a_{\boldsymbol{K}} \\ & + \Big[\frac{1}{2}U_0 n_0 + \frac{1}{2}(U_1 + U_2) n_0 \bar{\epsilon}_{\boldsymbol{K}}/J_0 \\ & + U_2 n_0 + n_0 U_3 (2 + \bar{\epsilon}_{\boldsymbol{K}}/J_0) \Big] \\ & \times \left(a_{\boldsymbol{K}} a_{-\boldsymbol{K}} + a_{\boldsymbol{K}}^\dagger a_{-\boldsymbol{K}}^\dagger \right) \Big\}, \quad (4) \end{aligned}$$

where $\sum'_{\boldsymbol{K}}$ denotes the summation for $\boldsymbol{K} \neq 0$ and $\bar{\epsilon}_{\boldsymbol{K}} = 2J_0 \sum_{j=1}^d \cos k_j a$ with a being the lattice constant of cubic lattices. The effective Hamiltonian can be diagonalized by a Bogoliubov transformation. This

implies that we define new creation and annihilation operators $b^{\dagger}_{\boldsymbol{K}}$ and $b_{\boldsymbol{K}}$ such that the effective Hamiltonian becomes diagonal

$$\begin{pmatrix} b_{\boldsymbol{K}} \\ b^{\dagger}_{-\boldsymbol{K}} \end{pmatrix} = \begin{bmatrix} u_{\boldsymbol{K}} & v_{\boldsymbol{K}} \\ v^{*}_{\boldsymbol{K}} & u^{*}_{\boldsymbol{K}} \end{bmatrix} \begin{pmatrix} a_{\boldsymbol{K}} \\ a^{\dagger}_{-\boldsymbol{K}} \end{pmatrix}. \tag{5}$$

To ensure that operators $b^{\dagger}_{\boldsymbol{K}}$ and $b_{\boldsymbol{K}}$ still obey the standard bosonic commutation relations, the following relation must be met

$$|u_{\boldsymbol{K}}|^2 - |v_{\boldsymbol{K}}|^2 = 1. \tag{6}$$

If we now substitute Eq. (5) into Eq. (4) and demand that the result reduces to the diagonal Hamiltonian

$$\begin{aligned} H_{\text{eff}} = & \left(-\frac{1}{2}U_0 n_0 - U_1 n_0 - \frac{3}{2}U_2 n_0 - \frac{1}{2}U_3 n_0\right) N_0 \\ & + \sum_{\boldsymbol{K}}{}' \left(A\nu^2_{\boldsymbol{K}} - 2Bu_{\boldsymbol{K}}\nu_{\boldsymbol{K}}\right) \\ & + \sum_{\boldsymbol{K}}{}' \left[A\left(u^2_{\boldsymbol{K}} + \nu^2_{\boldsymbol{K}}\right) - 4Bu_{\boldsymbol{K}}\nu_{\boldsymbol{K}}\right] \hat{b}^{\dagger}_{\boldsymbol{K}}\hat{b}_{\boldsymbol{K}}, \end{aligned} \tag{7}$$

where

$$\begin{aligned} A = & zJ_0 - \bar{\epsilon}_{\boldsymbol{K}} + U_0 n_0 + 2U_2 n_0 \bar{\epsilon}_{\boldsymbol{K}}/J_0 \\ & - U_2 n_0 + 7U_3 n_0 + 4U_3 n_0 \bar{\epsilon}_{\boldsymbol{K}}/J_0, \\ B = & \frac{1}{2}U_0 n_0 + \frac{1}{2}\left(U_1 + U_2\right) n_0 \bar{\epsilon}_{\boldsymbol{K}}/J_0 \\ & + U_2 n_0 + n_0 U_3 \left(2 + \bar{\epsilon}_{\boldsymbol{K}}/J_0\right), \end{aligned} \tag{8}$$

$u_{\boldsymbol{k}}$ and $v_{\boldsymbol{k}}$ must be the solutions of the following two equations:

$$\begin{aligned} & B\left(u^2_{\boldsymbol{K}} + \nu^2_{\boldsymbol{K}}\right) - Au_{\boldsymbol{K}}\nu_{\boldsymbol{K}} = 0, \\ & A\left(u^2_{\boldsymbol{K}} + \nu^2_{\boldsymbol{K}}\right) - 4Bu_{\boldsymbol{K}}\nu_{\boldsymbol{K}} = \hbar\omega_{\boldsymbol{K}}. \end{aligned} \tag{9}$$

Using the normalization condition in Eq. (6), the solution can be easily obtained

$$\begin{aligned} & \hbar\omega_{\boldsymbol{K}} = \sqrt{A^2 - 4B^2}, \\ & \nu^2_{\boldsymbol{K}} = \frac{1}{2}\left(\frac{A}{\hbar\omega_{\boldsymbol{K}}} - 1\right), \end{aligned} \tag{10}$$

where $\omega_{\boldsymbol{K}}$ is the excitation spectrum of the interacting Bose gas. As an example for one dimension it can be seen after a little algebra that

$$\omega_k = 2J_0 \sin\left|\frac{k}{2}\right| \sqrt{(1 - \cos k) + n_0 U_0/J_0}$$

in the case of weak interaction, i.e., $U_1 = U_2 = U_3 = 0$, the dispersion relation becomes linear $\omega_k \propto v_{\text{g}} k$ in the long wave-length limit $k \to 0$ with sound velocity $v_{\text{g}} = \sqrt{n_0 J_0 U_0}$, which coincides with the result.[18]

Next we calculate the depletion of the condensate. To obtain the condensate density n_0, we have to calculate the total density n with the effective Hamiltonian. The total density is expressed as

$$n = \frac{1}{N_s}\sum_{\boldsymbol{K}} \langle a^{\dagger}_{\boldsymbol{K}} a_{\boldsymbol{K}} \rangle_{H_{\text{eff}}}, \tag{11}$$

where the brackets $\langle\ \rangle_{H_{\text{eff}}}$ denote the expectation value as calculated with the effective Hamiltonian H_{eff}. For a Bose condensed gas, this density n includes two parts: the density n_0 associated with the macroscopic occupation of the one-particle ground-state, i.e., the condensate, and the density due to the occupation of the higher lying one-particle states. In this case, the density equals the sum of parameter n_0 and the density of non-condensate part determined by averaging over the quadratic fluctuations, which is expressed as a function of n_0

$$n = n_0 + \frac{1}{N_{\text{s}}}\sum_{\boldsymbol{K}}{}' \left[\left(u^2_{\boldsymbol{K}} + \nu^2_{\boldsymbol{K}}\right)\left\langle b^{\dagger}_{\boldsymbol{K}} b_{\boldsymbol{K}}\right\rangle_{H_{\text{eff}}} + \nu^2_{\boldsymbol{K}}\right]. \tag{12}$$

If we then use Eq. (9) and substitute the Bose distribution evaluated at $\hbar\omega_{\boldsymbol{K}}$ for $\langle b^{\dagger}_{\boldsymbol{K}} b_{\boldsymbol{K}}\rangle_{H_{\text{eff}}}$ we find that

$$n = n_0 + \frac{1}{N_{\text{s}}}\sum_{\boldsymbol{K}}{}' \left(\frac{A}{\hbar\omega_{\boldsymbol{K}}}\frac{1}{\mathrm{e}^{\beta\hbar\omega_{\boldsymbol{K}}} - 1} + \frac{A - \hbar\omega_{\boldsymbol{K}}}{2\hbar\omega_{\boldsymbol{K}}}\right). \tag{13}$$

Using the zero-temperature limit and taking the continuum limit for momenta $\boldsymbol{K}$ by using

$$\sum_{\boldsymbol{K}} \to V\int_{-\pi/a}^{\pi/a} \mathrm{d}\boldsymbol{K}/\left(2\pi\right)^d,$$

we arrive at the expression

$$n = n_0 + \frac{1}{2}\int_{-1/2}^{1/2} \mathrm{d}\boldsymbol{q}\left(\frac{A}{\hbar\omega_{\boldsymbol{K}}} - 1\right), \tag{14}$$

where $\boldsymbol{q} = 2\pi\boldsymbol{K}/a$ and n is the average total atom density per site. We can now obtain the condensate density by solving Eq. (13) for n_0 at a fixed value of n. Here we take $U_1 \approx U_2 \approx 0.02U_0$ according to the previous definition of Eq. (2), as can be evaluated roughly with Gaussian Wannier function and δ-function potential and justified reasonable for the close agreement with the experimental observation.[8,9] One can see that the condensate fraction n_0/n falls off rapidly and then tends to zero infinitely slowly with growing U_0/J_0 for BHM [dotted lines in Figs. 1(a) and 1(b)], however, the falling slope is small and remains a relatively large condensate fraction even when U_0/J_0 becomes sufficiently large for the EBHM [dashed lines in Figs. 1(a) and 1(b)]. The two-body interaction between bosons expels some particles from zero-momentum state to

other states.[19] The results show that the condensate fraction of EBHM is larger than that of BHM which is mainly due to the existence of additional interaction terms U_1, U_2, U_3, and suggests a pair condensate corresponding to pair superfluid.[20] However, the non-vanishing condensate fraction suggests that no phase transition occurs from superfluid to Mott insulator phase in two and three dimensions as predicted by Refs. [21] and [22], which is due to the fact that the Bogoliubov approach only approximately treats the interactions and cannot describe the large depletion of the condensate. Here the case in one dimension is not discussed for the existence of diverges, as illustrated in Ref. [22]. In the following we use the perturbation theory to obtain the rich phase diagrams within the EBHM.

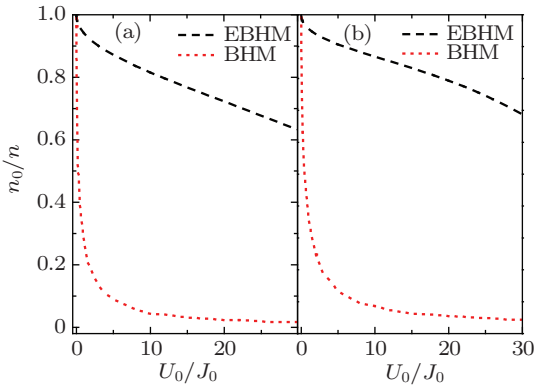


Fig. 1. (colour online) The condensate fraction n_0/n as a function of the dimensionless parameter U_0/J_0 with $n = 1$ for BHM (dotted lines) and EBHM (dashed lines): (a) a two-dimensional optical lattice and (b) a three-dimensional optical lattice.

4. Phase diagrams

The phase diagram of usual BHM with on-site approximation of boson–boson repulsion has been known for a long time.[7,22,24,25] The competition between the kinetic and potential energy terms leads to two phases: Mott-insulator (MI) phase when the kinetic energy is much smaller than the potential energy and a superfluid (SF) otherwise. Both of these phases, as well as the transition between them, have been successfully observed with ultracold Bose gases in optical lattices.[3,26–28] The phase diagrams of the model containing nearest-neighbor interactions have also been known[29–33] and two additional phases appear: charge density wave (CDW) phase and supersolid (SS) phase. Similar to the MI phase, the CDW phase is an insulator with an excitation gap and is incompressible. The main difference between the MI and CDW phases is that an integer number of bosons occupy every lattice site in the MI phase, while in the CDW phase the optical lattice loaded with bosonic atoms can be split into two sublattices with alternating atomic densities of n and $n+1$ analogous to the antiferromagnetic phase in the spin system. The SS phase is referred to as a phase with both long-range off-diagonal and diagonal order in an optical lattice, where the diagonal order breaks the translational symmetry of the lattice.[34] The quantum phases including MI, PSF, a normal SF and CDW states have been discussed in detail within an EBHM containing different kinds of correlated tunneling in Ref. [12]. In this paper we studied the system of our EBHM Hamiltonian (1) which extends the two-body interactions to nearest-neighbor sites. Since the coupling coefficients in Hamiltonian (1) are of high tunability, we can investigate the underlying physics in various parametric regions. From here we will neglect the effects of the U_3 term for simplicity.

4.1. Phase diagram with single-atom tunneling only

First we consider the case when U_2 is small compared to J where $J = J_0 - U_3(n_i + n_{i+1} - 1)$ is viewed as the single-atom tunneling amplitude. The Hamiltonian can be recast as

$$H = H_0 + H_{\rm I}, \tag{15}$$

$$H_0 = \sum_i \left(-\mu n_i + \frac{U_0}{2} a_i^\dagger a_i^\dagger a_i a_i + V a_i^\dagger a_{i+1}^\dagger a_{i+1} a_i \right),$$

$$H_{\rm I} = -J \sum_i \left(a_i^\dagger a_{i+1} + a_{i+1}^\dagger a_i \right), \tag{16}$$

where we replace $(U_1 + U_2)$ with V for convenience. To determine the phase boundaries we define the single-atom superfluidity order parameter as $\varphi_i = \langle a_i \rangle$. Here we restrict our analysis right from the state to real order parameter. A straightforward method is to use the mean-field approach perturbation in φ_i. Even though the mean-field theory becomes exact in the limit of infinite dimensions it can still capture the features of the phase diagrams qualitatively in low dimensions.[22,29,35] It is worthwhile pointing out that in an infinite dimension limit ($d \to \infty$) both tunneling amplitude J and the NN interactions V must scale inversely with d to ensure that zJ and zV are finite. Performing the mean-field decoupling of the Hamiltonian (14) with $a_i^\dagger a_{i+1} \approx a_i^\dagger \varphi_{i+1} + a_{i+1} \varphi_i - \varphi_i \varphi_{i+1}$ the nonlocal tunneling terms can be written as $H_{\rm I} =$

$-J\sum_i(a_i^\dagger + a_i)\varphi_i$. The phase boundaries between SF and MI, SS and CDW phases can be obtained as demonstrated in Ref. [36] based on the fact that the order parameter is finite ($\varphi_i \neq 0$) for the SF and SS ground states and it becomes zero for MI and CDW phase. We evaluate the order parameter $\varphi_i = \mathrm{Tr}(\rho a_i)$ at each site of the lattice. The partition function $Z = \mathrm{Tr}(\exp -\beta H)$ with β being the inverse of temperature can be approximated as $Z \approx \mathrm{Tr}(\exp -\beta H_0)$ after a Dyson expansion of the exponential to the lowest order. Thus the order parameter can be written through time-dependent perturbation theory in imaginary time

$$\begin{aligned}\varphi_i &= \mathrm{Tr}\{a_i \exp(-\beta H/Z)\} \\ &= \mathrm{Tr}\left\{a_i \exp(-\beta H_0)\mathscr{T}\exp\left[-\int_0^\beta H_{\mathrm{I}}(\tau)\,\mathrm{d}\tau\right]\right\}/Z \\ &\approx \mathrm{Tr}\left\{a_i \exp(-\beta H_0)\left[1-\int_0^\beta H_{\mathrm{I}}(\tau)\,\mathrm{d}\tau\right]\right\}/Z \\ &= -\sum_{g,g'}\int_0^\beta \mathrm{d}\tau\,\langle g|\,a_i\,\mathrm{e}^{\tau H_0}\,|g'\rangle\,\langle g'|\,H_{\mathrm{I}}\,\mathrm{e}^{-\tau H_0}\,|g\rangle\,,\end{aligned} \tag{17}$$

where the symbol $\mathscr{T}$ denotes time-ordering of the exponential, $H_{\mathrm{I}}(\tau) = \exp(\tau H_0)H_{\mathrm{I}}\exp(-\tau H_0)$ is time-dependent perturbation in the interaction representation and the sums of $|g'\rangle$ and $|g\rangle$ are complete sets of basis states of H_0. Taking the zero-temperature limit in the last line of Eq. (15) we can obtain after a little algebra

$$\begin{aligned}\varphi_i = J\bar{\varphi}_i\Bigg[&\frac{g+1}{U_0 g + V^{\mathrm{dip}} - \mu} \\ &- \frac{g}{U_0(g-1) + V^{\mathrm{dip}} - \mu}\Bigg]\end{aligned} \tag{18}$$

with $\bar{\varphi}_i = z\varphi$ being the sum of the nearest-neighbor order parameters and $V^{\mathrm{dip}} = zVg$ being the interaction of one atom placed at site i with the rest of the particles. The phase boundary can be determined due to the fact that the order parameter φ approaches zero near the phase boundary. We have

$$\begin{aligned}\mu_\pm = U_0\left(g-\frac{1}{2}\right) + zVg - \frac{1}{2}zJ \\ \pm\sqrt{U_0^2/4 - U_0(g+1/2)zJ + z^2J^2/4},\end{aligned} \tag{19}$$

where the subscript $\pm$ for μ denotes the upper (μ_+) and lower (μ_-) halves of the MI insulating regions of phase space, $g = \langle\hat{n}_i\rangle$ is the average occupancy which is chosen to minimize the on-site energy with the trivial limit $J = 0$ for a given μ. When $V = 0$ the results reduced to that of on-site BH model,[7,22] and the phase boundaries between CDW and SS phases can be expressed as

$$\begin{aligned}\frac{1}{(zJ)^2} = &\left[\frac{g_A+1}{U_0 g_A + zVg_B - \mu}\right. \\ &\left. - \frac{g_A}{U_0(g_A-1) + zVg_B - \mu}\right] \\ &\times\left[\frac{g_B+1}{U_0 g_B + zVg_A - \mu}\right. \\ &\left. - \frac{g_B}{U_0(g_B-1) + zVg_A - \mu}\right],\end{aligned} \tag{20}$$

where g_A and g_B are atomic densities in the two sublattices. The simple analytic solution for μ from Eq. (19) is not attainable and the numerical solution can be obtained for each of the CDW lobes separately. It is well known that for the case of an on-site interaction the phase diagram of BHM shows a series of lobes of the MI phase characterized by an integer number of particles per site. Once the nearest-neighbor interaction is introduced the CDW lobes appear between the Mott lobes, meanwhile another new phase, i.e., SS appear both in the SF and MI regions of phase diagram shown in Fig. 2. The integer filling $1, 2$ and fractional filling $1/2, 3/2$ form uniform Mott insulators and CDW state respectively. Further lobes appear for a longer range of interactions.[30] It is worthwhile pointing out that the Hamiltonian (14) can be mapped onto an effective spin XXZ model which has been investigated extensively on the mean-field level for the nearest neighbor.[29]

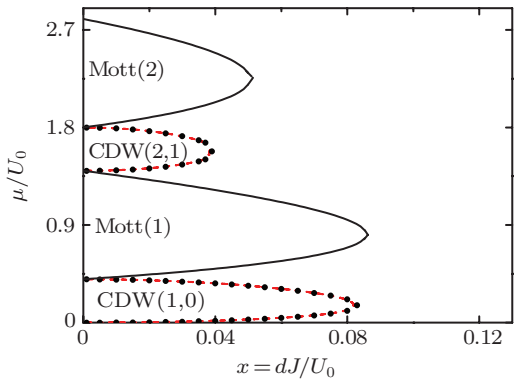


Fig. 2. (colour online) The (μ, J) phase diagram of the BHM with the additional nearest-neighbor interaction ($zV = 0.4U_0$) in infinite dimensions $d \to \infty$. The (red) dotted lines are the phase boundaries between CDW insulator and SS states and the (black) solid lines are the phase boundaries between MI and SF states.

4.2. Phase diagram with pair-tunneling only

In the case of a deep lattice when $J \ll J^{\rm P}$, where we substitute $J^{\rm P}$ for $U_2/2$ being the pair tunneling amplitude for convenience. It can be seen that the U_3-terms in fact suppresses the single particle tunneling between neighboring sites so that our assumption is realizable. The Hamiltonian reads

$$\begin{aligned} &H = H_0 + H_{\rm I}, \\ &H_0 = \sum_i \left[-\mu n_i + \frac{U_0}{2} n_i(n_i-1) + V n_i n_{i+1} \right], \\ &H_{\rm I} = J^{\rm P} \sum_i \left(A_i^\dagger A_{i+1} + A_{i+1}^\dagger A_i \right), \end{aligned} \tag{21}$$

where $A_i = a_i a_i$. Within mean-field theory we define the pair-superfluidity order parameter as $\psi_i = \langle A_i \rangle$. For the pair tunneling term $H_{\rm I}$ we can see its amplitude is always positive so we need to choose complex order parameters, i.e., take opposite signs on adjacent sites: $\langle A_i \rangle = \psi$, $\langle A_{i+1} \rangle = -\psi$ thus it can be guaranteed the concavity of the energy. So the original lattice must be split into two different sublattices denoted by A and B. The interacting part $H_{\rm I}$ can be rewritten as

$$\begin{aligned} H_{\rm I} = \; & J^{\rm P} \sum_{i\in A} \left(A_i^\dagger + A_i \right) \psi \\ & - J^{\rm P} \sum_{i\in B} \left(A_i^\dagger + A_i \right) \psi + J^{\rm P} N_{\rm s} \psi^2, \end{aligned} \tag{22}$$

where $N_{\rm s}$ is the number of the full lattice sites. Therefore Hamiltonian (19) is diagonal in a power series of ψ. The order parameter can be obtained by following the routines from the above section. We evaluate the order parameter $\psi_i = \langle A_i \rangle = {\rm Tr}(\rho A_i)$ at each site of the lattice. The partition function $Z = {\rm Tr}(\exp -\beta H)$ with β being the inverse of temperature can be approximated as $Z \approx {\rm Tr}(\exp -\beta H_0)$ after a Dyson expansion of the exponential to the lowest order. Thus the order parameter can be written through time-dependent perturbation theory in imaginary time

$$\begin{aligned} \psi_i &= {\rm Tr}[A_i \exp(-\beta H/Z)] \\ &\approx -\sum_{g,g'} \int_0^\beta {\rm d}\tau \, \langle g | \, a_i^2 \, {\rm e}^{\tau H_0} \, | g' \rangle \langle g' | \, H_{\rm I} \, {\rm e}^{-\tau H_0} \, | g \rangle \,, \end{aligned} \tag{23}$$

where $H_{\rm I}(\tau) = \exp(\tau H_0) H_{\rm I} \exp(-\tau H_0)$ is time-dependent perturbation in the interaction representation and the sums of $|g'\rangle$ and $|g\rangle$ are complete sets of the basis states of H_0. Taking the zero-temperature limit in the last line of Eq. (21) we can obtain after a little algebra

$$\begin{aligned} \psi_i = \; & J^{\rm P} \bar{\psi}_i \Bigg\{ \frac{(g+1)(g+2)}{[U_0(2g+1) - 2\mu] + 2V^{\rm dip}} \\ & - \frac{g(g-1)}{[U_0(2g-3) - 2\mu] + 2V^{\rm dip}} \Bigg\}. \end{aligned} \tag{24}$$

To determine the boundaries of the insulating lobes from Eq. (22) we define $\bar{\psi}_i = -z\psi$ being the sum of the nearest-neighbor order parameters and $V_i^{\rm dip} = zVg$ being the interaction of one atom placed at site i with the rest of the particles. Since the mean-field order parameter ψ approaches zero near the phase boundary, Eq. (22) can be satisfied only if

$$\begin{aligned} \frac{1}{zJ^{\rm P}} = \; & \frac{(g+1)(g+2)}{U_0(2g+1) + 2zVg - 2\mu} \\ & - \frac{g(g-1)}{U_0(2g-3) + 2zVg - 2\mu}. \end{aligned} \tag{25}$$

The solution for μ can be obtained easily

$$\begin{aligned} \mu_\pm = \; & U_0 \left(g - \frac{1}{2} \right) + zVg - zJ^{\rm P} \left(g + \frac{1}{2} \right) \\ & \pm \frac{1}{2} \sqrt{-4zJ^P \, U_0 \left(1 + g + g^2\right) + 4U_0^2 + \left(zJ^P\right)^2 \left(1 + 4g + 4g^2\right)}, \end{aligned} \tag{26}$$

where the subscript $\pm$ denotes the upper (μ_+) and lower (μ_-) halves of the MI regions of phase space. It can also be seen from Eq. (25) that the MI lobes are separated by zVg, but their shapes are independent of V. To determine the phase boundary between the CDW and PSS phases, from Eq. (22) we define $\psi_i = \psi_A$, $\bar{\psi}_i = z\psi_B$, $V_i^{\rm dip} = zVg_B$ for $i \in A$ sublattice, and define $\psi_j = \psi_B$, $\bar{\psi}_j = z\psi_A$, $V_j^{\rm dip} = zVg_A$ for $j \in B$ sublattice. This leads to two coupled equations for ψ_A and ψ_B. Since ψ_A and ψ_B approach zero near the phase boundary, Eq. (22) can be satisfied only if

$$\begin{aligned} \frac{1}{(zJ^{\rm P})^2} = \; & \Bigg[\frac{(g_A+1)(g_A+2)}{U_0(2g_A+1) + 2zVg_B - 2\mu} \\ & - \frac{g_A(g_A-1)}{U_0(2g_A-3) + 2zVg_B - 2\mu} \Bigg] \end{aligned}$$

$$\times\left[\frac{(g_B+1)(g_B+2)}{U_0(2g_B+1)+2zVg_A-2\mu}-\frac{g_B(g_B-1)}{U_0(2g_B-3)+2zVg_A-2\mu}\right]. \quad (27)$$

Simple analytic solutions to Eq. (25) are not attainable and numerical results can be obtained for each of the CDW lobes separately. The PSF and PSS regimes are outside the insulating lobes. The characteristics of the phase diagrams shown in Fig. 3 coincide qualitatively with the results of Ref. [12] by using Gutzwiller ansatz methods. The phase boundary between PSS and PSF is not attainable within the mean-field theory and more accurate methods are needed.

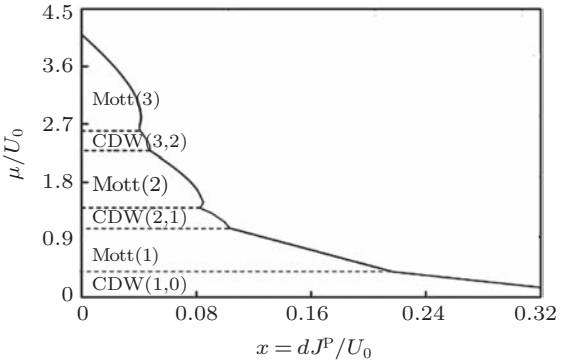


Fig. 3. The $(\mu, J^{\rm P})$ phase diagram of the EBHM with $zV = 0.4U_0$ in infinite dimensions $d \to \infty$. The phase boundaries separate the phases between MI and PSF, CDW and PSS.

4.3. Phase diagrams including both single-atom tunneling and pair-tunneling

In Ref. [37] an effective tunneling of pairs of bosonic atoms is obtained by virtue of an atom–molecule coupling system with large detuning but there exists pair tunneling directly in our Hamiltonian (1). In the case of $U_0 \gg (J^{\rm P}, J) \gg V$ the nearest-neighbor repulsive V-terms can be neglected. The Hamiltonian reads

$$\begin{aligned} H =& -\mu\sum_i n_i + \frac{U_0}{2}\sum_i a_i^\dagger a_i^\dagger a_i a_i \\ & - J\sum_i\left(a_i^\dagger a_{i+1} + a_{i+1}^\dagger a_i\right) \\ & + J^{\rm P}\sum_i\left(A_i^\dagger A_{i+1} + A_{i+1}^\dagger A_i\right). \end{aligned} \quad (28)$$

The above Hamiltonian contains two different kinds of tunneling terms. To investigate the SF to MI transition, we still employ the decoupling mean-field approximation in these tunneling terms. Assuming $\langle a_i\rangle = \varphi$ and $\langle A_i\rangle = \psi$ are two independent order parameters, we can obtain the "local" Hamiltonian

$$\begin{aligned} H =& H_0 + H_{\rm I}, \\ H_0 =& \sum_i\left(\frac{U_0}{2}a_i^{\dagger 2}a_i^2 - \mu a_i^\dagger a_i\right) + JN_{\rm s}\varphi^2 + J^{\rm P}N_{\rm s}\psi^2, \\ H_{\rm I} =& -\sum_i J\left(a_i + a_i^\dagger\right)\varphi + \sum_{i\in A} J^{\rm P}(A_i^\dagger + A_i)\psi \\ & - \sum_{i\in B} J^{\rm P}(A_i^\dagger + A_i)\psi. \end{aligned} \quad (29)$$

For the system containing a two-component order parameter, say (φ, ψ), the phases can be studied on the basis of Laudau's theory of phase transition. By employing the perturbation expansion, one can find that the free energy is expressed as

$$\begin{aligned} F(\varphi,\psi) =& \ a_0 + a_1\varphi^2 + a_2\psi^2 + a_3\varphi^2\psi \\ & + a_4\varphi^4 + a_5\psi^4 + a_6\varphi^2\psi^2 + \cdots. \end{aligned} \quad (30)$$

The explicit forms of a_i can be obtained by virtue of the method derived in Refs. [38] and [39]. We start from the MI phase of the highest symmetry with $\varphi = \psi = 0$ and proceed the other two phases: the pair-superfluidity phase PSF with a nonvanishing value of pair-superfluidity in the absence of SF, that is $\psi \neq 0$ but $\varphi = 0$; the normal SF phase with a nonvanishing value of superfluidity of the single atom in the absence of PSF, that is $\varphi \neq 0$ but $\psi = 0$. The phase diagrams can be obtained by minimizing the free energy with stability conditions taken into account. To minimize $F(\varphi, \psi)$, we use the criteria $\partial F/\partial x = 0$, $(x = \varphi, \psi)$ which yields

$$\begin{aligned} &\varphi\left(2a_1 + 2a_3\psi + 4a_4\varphi^2 + \cdots\right) = 0, \\ &\psi\left(2a_2 + 4a_5\psi^2 + \cdots\right) + a_3\varphi^2 = 0. \end{aligned} \quad (31)$$

From Eqs. (29) we can see if $\psi = 0$, φ may be nonzero determined by $a_1 + 2a_4\varphi^2 = 0$ for a_3 always being zero due to the fact that there is opposite-sign pair-superfluidity order parameter between neighboring sites, which means that the system can be in a phase with $\psi = 0$ and $\varphi^2 = -a_1/2a_4$. Meanwhile when $\varphi = 0$, ψ may be nonzero and determined by $a_2 + 2a_5\psi^2 = 0$, which means that the system can be in PSF phase with $\varphi = 0$ and $\psi^2 = -a_2/2a_5$. Figure 4 shows the (μ, J) phase diagram when $\psi = 0$, in which the the contour plots depict the value of SF order parameter and the solid line denotes the boundary between MI and SF phases. One can see the contour plots cover the portions of the Mott lobes, but however in such parameter regions the ground state is still

the Mott phase and the SF ($\varphi \neq 0$) phase is unstable. Figure 5 shows the (μ, J^P) phase diagram when $\varphi = 0$ in which the contour plots represent the value of the PSF order parameter. One can see that the Mott lobes fit the borders of the PSF phase exactly and the contour plots shows a stable PSF phase.

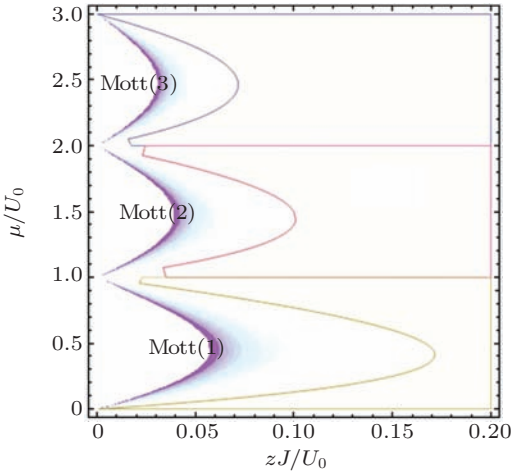


Fig. 4. (colour online) The (μ, J) phase diagram of Hamiltonian (27). The contour plots depict SF order parameter φ and the solid line denotes the boundary between MI and SF phases.

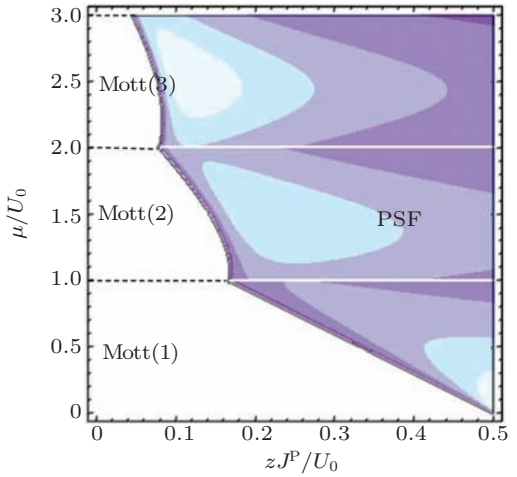


Fig. 5. (colour online) The $(\mu, J^{\rm P})$ phase diagram of Hamiltonian (27). The contour plots depict the value of PSF order parameter ψ.

5. Conclusion

In conclusion we have investigated the excitation spectrum and the depletion of the condensate of Bose gases in optical lattices with two-body interactions of nearest-neighbors characterized by a PSF within the mean-field theory. The result shows that there exists a pair condensate as well as a single particle condensate. The rich phase diagrams with quantum phases such as MI, SF, CDW, PSF, and PSS are discussed under various parametric conditions. As for the experimental observability, the noise correlation technique can provide an observable signature to detect and characterize the different quantum phases.[37,40] It is worthwile pointing out that the mean-field theory cannot be used to calculate the phase boundary between two compressible phases, e.g., the SS-to-SF and PSS-to-PSF transitions and more accurate methods are needed.

References

[1] Greiner M, Bloch I, Mandel O, Hänch T W and Esslinger T 2001 *Phys. Rev. Lett.* **87** 160405
[2] Orzel C, Tuchman A K, Fenselau M L, Yasuda M and Kasevich M A 2001 *Science* **291** 2386
[3] Greiner M, Mandel O, Esslinger T, Hänsch T W and Bloch I 2002 *Nature* **415** 39
[4] Greiner M, Mandel O, Hänsch T W and Bloch I 2002 *Nature* **419** 51
[5] Anglin J R and Ketterle W 2002 *Nature* **416** 211
[6] Jaksch D, Bruder C, Cirac J I, Gardiner C W and Zoller P 1998 *Phys. Rev. Lett.* **81** 3108
[7] Fisher M P A, Weichman P B, Grinstein G and Fisher D S 1989 *Phys. Rev.* B **40** 546
[8] Liang J Q, Liu J L, Li W D and Li Z J 2009 *Phys. Rev.* A **79** 033617
[9] Fölling S, Trotzky S, Cheinet P, Feld M, Saers R, Widera A, Müller T and Bloch I 2007 *Nature* **448** 1029
[10] Duan L M, Demler E and Lukin M D 2003 *Phys. Rev. Lett.* **91** 090402
[11] Kuklov A B and Svistunov B V 2003 *Phys. Rev. Lett.* **90** 100401
[12] Eckholt M and García-Ripoll J J 2009 *New J. Phys.* **11** 093028
[13] Park J and Sim H S 2010 *Phys. Rev.* B **82** 235318
[14] Wysokiński K I 2010 *Phys. Rev.* B **82** 115423
[15] Zhou T 2011 *Phys. Rev. Lett.* **106** 167001
[16] Longhi S 2011 *Phys. Rev.* A **83** 043835
[17] Wang Y M and Liang J Q 2010 *Phys. Rev.* A **81** 045601
[18] Liang J J, Liang J Q and Liu W M 2003 *Phys. Rev.* A **68** 043605
[19] Pethick C J and Smith H 2008 *Bose–Einstein Condensation in Dilute Gases* 2nd edn. (Cambridge: Cambridge University Press) p. 231
[20] Radzihovsky L, Park J and Weichman P B 2004 *Phys. Rev. Lett.* **92** 160402
[21] Sheshadri K, Krishnamurthy H R, Pandit R and Ramakrishnan T V 1993 *Europhys. Lett.* **22** 257
[22] Oosten D V, Straten P V and Stoof H T C 2001 *Phys. Rev.* A **63** 053601
[23] Wang Y J, Liu X F and Han J R 2009 *Chin. Phys.* B **18** 5301
[24] Freericks J K and Monien H 1996 *Phys. Rev.* B **53** 2691
[25] Capogrosso-Sansone B, Söyler S G, Prokof'ev N V and Svistunov B V 2008 *Phys. Rev.* A **77** 015602
[26] Spielman I B, Phillips W D and Porto J V 2007 *Phys. Rev. Lett.* **98** 080404

[27] Spielman I B, Phillips W D and Porto J V 2008 *Phys. Rev. Lett.* **100** 120402

[28] Gerbier F, Trotzky S, Fölling S, Schnorrberger U, Thompson J D, Widera A, Bloch I, Pollet L, Troyer M, Sansone B C, Prokof'ev N V and Svistunov B V 2008 *Phys. Rev. Lett.* **101** 155303

[29] Van Otterlo A, Wagenblast K H, Baltin R, Bruder C, Fazio R and Schön G 1995 *Phys. Rev.* B **52** 16176

[30] Bruder C, Fazio R and Schön G 1993 *Phys. Rev.* B **47** 342

[31] Niyaz P, Scalettar R T, Fong C Y and Batrouni G G 1994 *Phys. Rev.* B **50** 362

[32] Kühner T D, White S R and Monien H 2000 *Phys. Rev.* B **61** 12474

[33] Kovrizhin D L, Pai G V and Sinha S 2005 *Europhys. Lett.* **72** 162

[34] Leggett A J 1970 *Phys. Rev. Lett.* **25** 1543

[35] Ohliger M and Pelster A 2008 *arXiv*: 0810.4399v1

[36] Iskin M and Freericks J K 2009 *Phys. Rev.* A **79** 053634

[37] Zhou X F, Zhang Y S and Guo G C 2009 *Phys. Rev.* A **80** 013605

[38] Messiah A 1962 *Quantum Mechanics* Vol. II (Amsterdam: North-Holland) p. 686

[39] Dos Santos F E A and Pelster A 2009 *Phys. Rev.* A **79** 013614

[40] Scarola V W, Demler E and Das Sarma S 2006 *Phys. Rev.* A **73** 051601